Laser-Induced Charge-Density-Wave Transient Depinning in Chromium

V. L. R. Jacques,[1,*] C. Laulhé,[2,3] N. Moisan,[1] S. Ravy,[1] and D. Le Bolloc'h[1]
[1]Laboratoire de Physique des Solides, CNRS, Univ. Paris-Sud, Université Paris-Saclay, 91405 Orsay Cedex, France
[2]Synchrotron Soleil, L'Orme des Merisiers, Saint-Aubin, BP 48, 91192 Gif-sur-Yvette Cedex, France
[3]Univ. Paris-Sud, Université Paris-Saclay, 91405 Orsay Cedex, France
(Received 11 May 2016; revised manuscript received 3 August 2016; published 3 October 2016)

We report on time-resolved x-ray diffraction measurements following femtosecond laser excitation in pure bulk chromium. Comparing the evolution of incommensurate charge-density-wave (CDW) and atomic lattice reflections, we show that, a few nanoseconds after laser excitation, the CDW undergoes different structural changes than the atomic lattice. We give evidence for a transient CDW shear strain that breaks the lattice point symmetry. This strain is characteristic of sliding CDWs, as observed in other incommensurate CDW systems, suggesting the laser-induced CDW sliding capability in 3D systems. This first evidence opens perspectives for unconventional laser-assisted transport of correlated charges.

DOI: 10.1103/PhysRevLett.117.156401

Understanding the interplay between spin, charge, and lattice is a major issue in condensed matter. Chromium is a typical system having complex electronic and magnetic ground states despite a basic crystallographic structure [1]. Below 311 K, a spin density wave (SDW) appears together with a charge-density-wave (CDW) and strain wave modulation, the period of the SDW being twice that of the CDW. In bulk chromium, the ratio of the atomic lattice and CDW periods is incommensurate. In principle, this implies that energetically equivalent states are found whatever the position of the CDW with respect to the atomic lattice. In some low-dimensional systems, this translational invariance leads to nonlinear transport properties due to CDW sliding [2]. However, such a phenomenon has never been observed in 3D systems like chromium [3].

Systems subjected to external driving forces in disordered media share universal behaviors. For various systems, such as surfaces, vortices in type-II superconductors [4], or magnetic domain walls [5], similar regimes are sequentially observed—pinning, creep and flow—depending on the pinning strength compared to the applied force magnitude. The case of periodic systems, like CDWs, is peculiar. They are generally found in low-dimensional materials, characterized by strong structural anisotropy, when a periodic lattice distortion allows a major decrease of the electron energy thanks to a gap opening, resulting in a static modulation of the electron density [6]. CDWs are pinned to the lattice either because of local impurity potentials or commensurability effects between the lattice and the CDW periodicities. Depinning thus requires the CDW and lattice periods to be incommensurate, i.e., to have an irrational ratio. When it takes place, the collective transport of charges is detectable through the non-Ohmic behavior of the current-voltage characteristics, as well as an additional ac voltage. This effect has been observed in several quasi-one-dimensional systems like $NbSe_3$ [2] and the blue bronze [7]. More recently, quasi-2D CDW systems were also found to have this ability [8,9] but CDW sliding has never been observed in 3D materials so far.

The presence of a CDW in an isotropic 3D metal like chromium is exceptional. In the bulk, this metal indeed displays incommensurate DWs although its structure is cubic and monoatomic, with hardly any anisotropy of its properties [1]. It was the first metal identified to display a linear incommensurate SDW with reduced wave vector δ varying between 0.037 and 0.048 reciprocal lattice units (r.l.u.) as a function of temperature, due to itinerant $3d$ electrons [10]. Associated charge harmonics were first predicted [11] and later evidenced [12]. The coexistence of both CDW and SDW in chromium has led to extensive studies to unravel the coupling between spin, charge, and lattice [10–18].

A temporal study of these components can provide valuable information about their interdependency. Contrary to many other CDW systems [19–26], the ultrafast dynamics of chromium has never been studied in bulks. Femtosecond reflectivity experiments on thin films showed that the ultrafast electronic response is well accounted for by the two-temperature model [27,28], which was confirmed by a recent diffraction study of a commensurate CDW in a Cr film as well [29].

In this work, the CDW modulation (and the superimposed periodic lattice distortion) and the average lattice were studied as a function of time after femtosecond laser excitation by picosecond time-resolved x-ray diffraction in a bulk. The strength of this technique is its wave vector selectivity, which allows us to track the time-dependent behavior of the CDW and average lattice independently. The experiment was performed at the CRISTAL beam line of the SOLEIL synchrotron, in the eight-bunch operation mode. The setup used for the experiment is shown in Fig. 1(a).

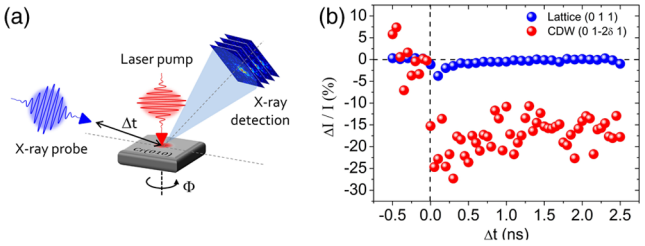

FIG. 1. (a) Experimental setup scheme. The Cr(010) single crystal is excited by a 800 nm femtosecond laser pulse and probed by a 70 ps x-ray pulse sent with a temporal delay Δt after laser excitation, in 1° grazing-incidence geometry. (b) Intensity variations of the 0 1 1 Bragg reflection and of the 0 1-2δ 1 satellite reflection associated to the lattice and the CDW, respectively, recorded at fixed position of sample and detector during the first nanoseconds following laser excitation.

The temporal resolution of this experiment was given by the x-ray pulse duration of 76 ps full width at half maximum (FWHM). A multi-Q (010) Cr single crystal was mounted on the six-circle diffractometer of the beam line, and excited with 30 fs infrared laser pulses (at 1.55 eV/800 nm) synchronized with the x-ray pulses at a repetition rate of 1 kHz. The laser beam impinged the sample perpendicular to its (010) surface with a spot size radius of 2 mm FWHM, yielding a fluence of 6.2 mJ/cm^2. The 0 1-2δ 1 reflection associated to the CDW was probed with 7.15 keV x-ray pulses (wavelength 1.734 Å), far from the chromium K-edge energy ($E_K = 5.988$ keV). The 0 1 1 reflection was measured to track variations of the lattice structure. In order to match the effective penetration depth of x-rays with the 70 nm laser penetration depth along the direction normal to the sample's surface, x-rays were set to impinge the sample at a grazing angle $\theta_i = 1°$—above the 0.414° critical angle of chromium at this energy—[see Fig. 1(a)]. The x-ray beam footprint was ~1.7 mm along the incident beam direction and 0.5 mm in the perpendicular direction. Detection was performed using a 2D pixel detector (XPAD3.2 with 130 μm pixels) located at 387 mm from the sample, leading to a resolution of 1.217×10^{-3} Å^{-1} close to the 0 1 1 position in reciprocal space. Single bunches were selected by synchronizing a 100 ns detector counting gate with the laser excitation pulse. Each pump-probe measurement was obtained by summing 1000 events. The sample was cooled down using a He blower refrigerator to reach temperatures from 50 to 300 K without screening the laser and x-ray beams on the sample. The working temperature was set to 140 K. When the laser was switched on, the CDW reflection was found at a different position than the one measured without laser in reciprocal space, corresponding to an overall temperature increase of around 30 K.

Figure 1(b) shows the diffracted intensity measured as a function of pump-probe delay at a temperature of 140 K, at two fixed positions in reciprocal space, 0 1-2δ 1 and 0 1 1. These positions correspond to the CDW and underlying cubic crystal structure as measured before laser excitation. The time evolution of diffracted intensities shown in Fig. 1(b) reflects all at once possible sources of structure factor changes, Debye-Waller contribution, and diffraction peak position. Nevertheless, this measurement provides valuable information. First, while intensity variations of the 0 1 1 Bragg reflection keep smaller than 5%, a 30% intensity drop is observed for the CDW satellite peak during the first 250 ps following laser excitation. Second, the initial state is not fully recovered after $\Delta t = 2.5$ ns. The lattice expansion is very small in chromium in this temperature range ($\Delta a/a \sim 2 \times 10^{-4}$) and not measurable with the resolution of our experiment limited by the 130 μm pixel size of the detector leading to $\Delta q/q \sim 4 \times 10^{-4}$. The intensity variation of the 0 1 1 Bragg reflection cannot be attributed to a Debye-Waller contribution, that would lead to a 0.5% intensity decrease for a 30 K temperature variation [30], which is the measured heating of the sample at this delay, as shown in the following. Thus, the 0 1 1 intensity variation recorded at 0.1 ns can only be attributed to a remaining strain due to thermal propagation, that ends after ~0.5 ns.

In order to get full information on the CDW satellite peak position in reciprocal space, we performed azimuthal angle Φ scans for different pump-probe delays [see Fig. 1(a)]. The time evolutions of the CDW peak position and FWHM are plotted in Figs. 2(b) and 2(c), respectively.

At $\Delta t = 0.1$ ns after laser excitation, the CDW peak position is shifted with respect to its negative delay value, and accompanied by a clear peak broadening. The diffraction angle and FWHM then continuously evolve until

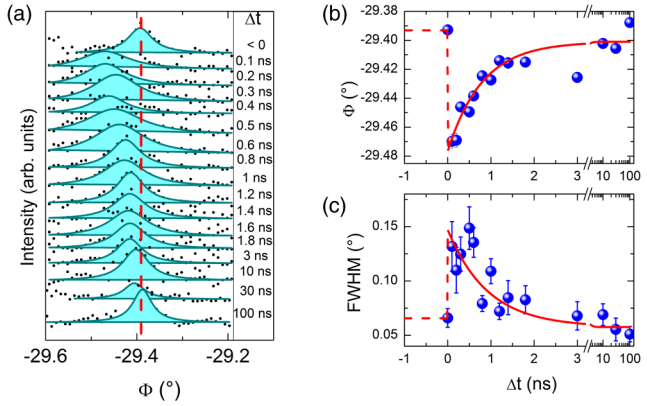

FIG. 2. (a) Φ scans as a function of time delay Δt, obtained by integrating the signal on the detector at 140 K. The dots are measured points and the blue filled areas bound by solid lines are fit of the experimental data. The position of the maximum measured at negative delays is indicated by the red dashed line. (b) Evolution of the central position and (c), of the FWHM of the CDW reflection extracted from the fits shown in (a) as a function of time delay Δt (blue dots). The red solid line is exponential fit to the data, and the red dashed lines are guides to the eye.

recovering their initial value at $\Delta t \sim 100$ ns. Diffraction angle and FWHM follow similar exponential evolution with a characteristic time of 3 ns to recover 90% of the initial values. Maximum changes are found at $\Delta t = 0.1$ ns with a peak shifted by 0.08° and twice as broad as before excitation. The corresponding correlation lengths are 0.4 μm in the initial state and 0.2 μm at $\Delta t = 0.1$ ns. In comparison the 0 1 1 Bragg peak position and shape hardly change (see Supplemental Material [31]). This measurement first shows that the CDW is excited by the laser pulse in a time shorter than the 70 ps time resolution of this experiment and is then followed by a much longer relaxation process involving a strong change of CDW correlation lengths.

The most surprising point is that this relaxation process also involves a deep modification of the CDW structure. The detailed q analysis reveals a peculiar behavior of the CDW wave vector during this relaxation, involving a dilatation followed by a contraction as well as a tilt. This is clearly observed by vertical shifts $\Delta\delta$ on the detector corresponding to variations of the wave vector longitudinal component δ and horizontal shifts $\Delta\alpha$ associated to tilts of the CDW wave vector [see Fig. 3(a)]. The temporal evolution of $\Delta\delta$ and $\Delta\alpha$ extracted from the images recorded at the maximum intensity of the Φ scan for each delay is plotted in Figs. 3(b)–3(c).

The 1.55 eV laser pulse energy is much larger than the SDW gap of chromium of ~150 meV. By analogy with other CDW systems, electronic excitations above the gap are expected as well as a subsequent decrease of the gap [21,24,32]. However, these athermal processes occurring within the first tens of femtoseconds cannot be studied with the present time resolution.

The temporal evolution follows three successive steps: (1) from 0 to 500 ps, the longitudinal component $\Delta\delta$ abruptly changes, (2) from 500 ps to 10 ns a strong $\Delta\alpha$ variation induces a lattice point symmetry breaking, and (3) relaxation occurs after 10 ns. During the first step, the longitudinal component of the CDW wave vector δ decreases in less than 70 ps, and corresponds to a CDW expansion in quantitative agreement with the Φ time dependence shown in Fig. 2(b). In the relaxed state, $\delta \sim 0.0447$ r.l.u., whereas at $\Delta t = 0.1$ ns, $\delta = 0.0422$ r.l.u. This corresponds to an effective temperature increase of 30 K due to laser excitation according to thermodynamical measurements [14]. The CDW in the excited part of the sample expands faster than 70 ps, while in the nonexcited regions it keeps the same period, with a nearly 6% mismatch between the two regions. The huge associated CDW strain must lead to the nucleation of necessary dislocations in the boundary region and glide during the out-of-equilibrium process to accommodate for the strain variation [33]. This mechanism could be responsible for the decrease of the CDW correlation length at the nanosecond time scale.

Interestingly enough, the evolution from 500 ps to 10 ns clearly shows that the return to equilibrium does not simply

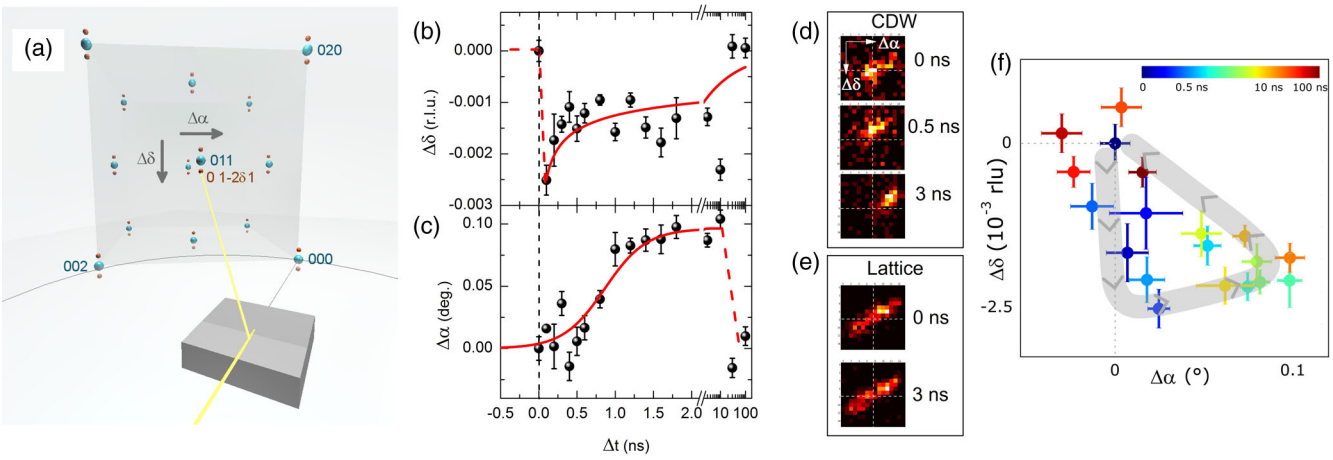

FIG. 3. (a) Sketch to scale of the Ewald construction (see Supplemental Material [31]), showing the incident beam impinging the sample with a grazing angle and the reciprocal space geometry when the 0 1-2δ 1 reflection is in diffraction condition. Blue dots are reciprocal space points associated to the lattice, and orange ones to the CDW. CDW wave vector variations $\Delta\delta$ appear along the vertical direction of recorded images, and tilts $\Delta\alpha$ along the horizontal direction. (b) Variations of the CDW wave vector modulus δ and (c) of its angle α relative to their values at negative delay, extracted from the peak position on the detector taken on the maximum of the Φ scans shown in Fig. 2(a). Black dots are experimental data, red lines are fits to the data. (d) CDW reflection recorded on the 2D detector at $\Delta t = 0$, 0.5, and 3 ns at the maximum Φ. (e) 0 1 1 lattice reflection recorded at $\Delta t = 0$ and 3 ns at the same position of the sample as the CDW shown in (d). No position variation is observed for the lattice reflection. (f) Evolution of the CDW reflection in reciprocal space for delays between 0 and 100 ns. Each dot represents the CDW reflection center of mass as recorded on the 2D detector, and the color code indicating the delay is shown on the colorscale on the top of the image. Horizontal and vertical error bars are given by the fit of the peak projections along the vertical and horizontal directions of the detector. The gray line depicts the global trajectory of the CDW peak on the detector, and arrows show the direction of time.

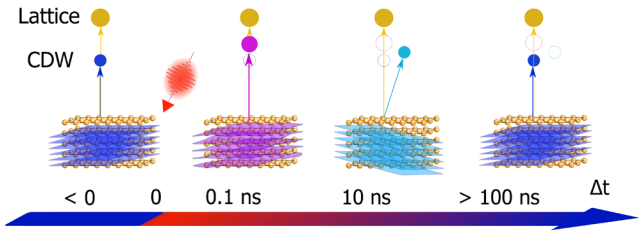

FIG. 4. Time evolution of the system after laser excitation. The bottom time line specifies the relative time delay between x-ray and laser pulses. Blue portions depict the equilibrium state of the system and red ones to excited warmer states. The probed sample portion is depicted in the middle line, and is not to scale. The yellow ball grid describes the atomic lattice and the probed CDW domains oriented along the surface normal are the parallel sheets (not to scale), blue in the thermodynamical state ($\Delta t < 0$ and $\Delta t > 100$ ns), purple at $\Delta t = 0.1$ ns, and light blue at $\Delta t = 10$ ns. In the upper part of the figure, the time evolution of the lattice and CDW reflection are drawn and follow the orientation and period changes of the structures in real space and at each delay. The open circles in dashed color lines represent the peak positions at earlier delays. At negative delays, the CDW has long correlation lengths, and is oriented along the surface normal. At $\Delta t = 1$ ns, the CDW period is larger, and its wave fronts are distorted, leading to shorter correlation lengths. At $\Delta t = 10$ ns, the wave fronts are less distorted, the CDW period is changing towards its equilibrium period, but a rotation of its wave vector occurs, which breaks the system symmetry. The system is back to its original state after 100 ns.

involve the reversible contraction of the CDW and a recovery of initial correlation lengths, but that an intermediate step takes place. In this temporal window, the CDW wave vector continuously rotates up to 0.08° from 0.5 to 10 ns, while no change of the fundamental Bragg refection is observed [Fig. 3(e)]. A real-space picture of the evolution of the system after laser excitation is shown in Fig. 4.

This substantial bending is not expected in the CDW relaxation process as it breaks the orientational symmetry of the CDW with respect to the lattice: the CDW wave vector is no more collinear with the [0 1 0] direction of the cubic lattice. This result has a fundamental implication since, despite the CDW incommensurability that implies translational invariance of the system, no CDW depinning has ever been observed in chromium [3].

All possible experimental asymmetries prove inconsistent with the observed phenomenon. A first possible asymmetry in the experiment is the laser incidence on the sample, which could slightly deviate from the sample normal. The incidence angle incertitude is 1° around the normal incidence. With a 2 mm diameter spot, this corresponds to a 35 μm propagation difference, and thus to 100 fs time difference, between excited regions on both sides of the laser spot, incompatible with the time scales involved here. Strain wave propagation cannot be invoked either, as their propagation at $\sim 5 \times 10^3$ m/s within the 100 nm probed region takes place within 20 ps, much faster than the ns time scale at which the CDW tilt occurs.

The phenomenon involved in the observed symmetry breaking is linked to a shear of the CDW as predicted theoretically [34] and observed in sliding CDWs [35]. The observed shear is most probably related to the deformation of the elastic CDW in the presence of pinning centers [34]. The exact nanometric CDW configuration is not accessible from this diffraction experiment averaging over such a large probed volume. However, several hypotheses can be made. A first possible scenario relies on CDW pinned with several pinning centers randomly distributed in the bulk. After laser excitation, a collective depinning is observed leading to a global shear of the CDW as expected in the strong pinning theory [36]. A second scenario relies on the interaction of the CDW with a single strong pinning center, such as a large grain boundary, localized close to the probed volume.

We show in this Letter several important results. The decoupling of the CDW from the atomic lattice has been expected in chromium for a long time because it displays an incommensurate CDW which is a necessary condition to observe CDW sliding. In previous experiments performed on chromium thin films, in which the CDW is commensurate and thus pinned on the atomic lattice, this effect was not observed [29]. However, CDW depinning had never been observed in bulk chromium either mainly because it is an excellent metal in which an anomaly of the current-voltage characteristic is hard to measure. Here, we highlight the possibility to depin the CDW from the host lattice in chromium, not with an external dc current as for usual sliding CDW systems, but with an ultrashort laser excitation. The observed shear between 0.5 and 10 ns is similar to that observed in the sliding CDW of the quasi-2D system $TbTe_3$ [8,9]. This first observation of depinning in a 3D CDW system provides new perspectives in terms of collective charge transport using laser excitations.

The authors acknowledge Synchrotron-SOLEIL for providing beam time and for support during the experiment.

*vincent.jacques@u-psud.fr

[1] E. Fawcett, Rev. Mod. Phys. **60**, 209 (1988).
[2] P. Monceau, N. P. Ong, A. M. Portis, A. Meerschaut, and J. Rouxel, Phys. Rev. Lett. **37**, 602 (1976).
[3] I. D. Parker and A. Zettl, Phys. Rev. B **44**, 5313 (1991).
[4] T. Giamarchi and P. Le Doussal, Phys. Rev. B **52**, 1242 (1995).
[5] A. Thiaville, Y. Nakatani, J. Miltat, and Y. Suzuki, Europhys. Lett. **69**, 990 (2005).
[6] P. Monceau, Adv. Phys. **61**, 325 (2012).
[7] J. Dumas, C. Schlenker, J. Marcus, and R. Buder, Phys. Rev. Lett. **50**, 757 (1983).
[8] A. A. Sinchenko, P. Lejay, and P. Monceau, Phys. Rev. B **85**, 241104 (2012).

[9] D. Le Bolloc'h, A. A. Sinchenko, V. L. R. Jacques, L. Ortega, J. E. Lorenzo, G. A. Chahine, P. Lejay, and P. Monceau, Phys. Rev. B **93**, 165124 (2016).
[10] A. W. Overhauser, Phys. Rev. **128**, 1437 (1962).
[11] C. Young and J. Sokoloff, J. Phys. F **4**, 1304 (1974).
[12] Y. Tsunoda, M. Mori, N. Kunitomi, Y. Teraoka, and J. Kanamori, Solid State Commun. **14**, 287 (1974).
[13] L. M. Corliss, J. M. Hastings, and R. J. Weiss, Phys. Rev. Lett. **3**, 211 (1959).
[14] S. A. Werner, A. Arrott, and H. Kendrick, Phys. Rev. **155**, 528 (1967).
[15] W. Cowan, J. Phys. F **8**, 423 (1978).
[16] V. L. Jacques, D. L. Bolloc'h, S. Ravy, C. Giles, F. Livet, and S. B. Wilkins, Eur. Phys. J. B **70**, 317 (2009).
[17] V. L. R. Jacques, E. Pinsolle, S. Ravy, G. Abramovici, and D. Le Bolloc'h, Phys. Rev. B **89**, 245127 (2014).
[18] P. Evans, E. Isaacs, G. Aeppli, Z. Cai, and B. Lai, Science **295**, 1042 (2002).
[19] R. Yusupov, T. Mertelj, V. V. Kabanov, S. Brazovskii, P. Kusar, J.-H. Chu, I. R. Fisher, and D. Mihailovic, Nat. Phys. **6**, 681 (2010).
[20] J. Demsar, K. Biljakovic, and D. Mihailovic, Phys. Rev. Lett. **83**, 800 (1999).
[21] A. Tomeljak, H. Schafer, D. Stadter, M. Beyer, K. Biljakovic, and J. Demsar, Phys. Rev. Lett. **102**, 066404 (2009).
[22] F. Schmitt *et al.*, Science **321**, 1649 (2008).
[23] H. Y. Liu, I. Gierz, J. C. Petersen, S. Kaiser, A. Simoncig, A. L. Cavalieri, C. Cacho, I. C. E. Turcu, E. Springate, F. Frassetto *et al.*, Phys. Rev. B **88**, 045104 (2013).
[24] M. Eichberger, H. Schafer, M. Krumova, M. Beyer, J. Demsar, H. Berger, G. Moriena, G. Sciaini, and R. J. D. Miller, Nature (London) **468**, 799 (2010).
[25] T. Huber, S. Mariager, A. Ferrer, H. Schäfer, J. Johnson, S. Grübel, A. Lübcke, L. Huber, T. Kubacka, C. Dornes *et al.*, Phys. Rev. Lett. **113**, 026401 (2014).
[26] C. Laulhé *et al.*, Physica (Amsterdam) **460B**, 100 (2015).
[27] H. Hirori, T. Tachizaki, O. Matsuda, and O. B. Wright, Phys. Rev. B **68**, 113102 (2003).
[28] S. D. Brorson, A. Kazeroonian, J. S. Moodera, D. W. Face, T. K. Cheng, E. P. Ippen, M. S. Dresselhaus, and G. Dresselhaus, Phys. Rev. Lett. **64**, 2172 (1990).
[29] A. Singer *et al.*, Phys. Rev. B **91**, 115134 (2015).
[30] S. Pal, J. Chem. Phys. **60**, 2741 (1974).
[31] See Supplemental Material at http://link.aps.org/supplemental/10.1103/PhysRevLett.117.156401 for information on the experimental geometry, raw detector images, and data analysis.
[32] S. L. Johnson, P. Beaud, E. Vorobeva, C. J. Milne, E. D. Murray, S. Fahy, and G. Ingold, Acta Crystallogr. Sect. A **66**, 157 (2010).
[33] K. Parlinski, Phys. Rev. B **35**, 8680 (1987).
[34] D. Feinberg and J. Friedel, J. Phys. II (France) **49**, 485 (1988).
[35] A. F. Isakovic, P. G. Evans, J. Kmetko, K. Cicak, Z. Cai, B. Lai, and R. E. Thorne, Phys. Rev. Lett. **96**, 046401 (2006).
[36] P. A. Lee and T. M. Rice, Phys. Rev. B **19**, 3970 (1979).